Korean J. Chem. Eng., **25**(6), 1518-1523 (2008)

Adsorption and desorption characteristics of CF_4 on fixed bed column

Sung-Sup Suh*, Neung Gyun Ahn*, and Byung-Ki Na,†**

*Department of Chemical Engineering, Hongik University, 72-1 Sangsu-dong, Mapo-gu, Seoul 121-791, Korea
**School of Chemical Engineering, Chungbuk National University, 12 Gaesin-dong, Heungduk-gu, Chungbuk 361-763, Korea
(*Received 18 February 2008 • accepted 29 May 2008*)

Abstract−Adsorption and desorption characteristics of CF_4, which is considered a significant global warming compound, were experimentally investigated. Dynamic behavior of feed gas mixture of CF_4 and N_2 was observed by breakthrough curve. Effects of CF_4 concentrations in the feed gas were investigated, and three pressurization methods were compared. Desorption experiments were carried out using vacuum blowdown and purge. Desorption curves with various N_2 flow rates, feed compositions, and purge time were obtained. The enrichment factor was high for low concentration of CF_4. However, the time required for complete desorption was independent of CF_4 concentration. In the operation of separate vacuum blowdown and purge steps, a short period of vacuum blowdown followed by the purge step was effective.

Key words: Adsorption, CF_4, Global Warming Gas, Breakthrough Curve, Desorption Curve

INTRODUCTION

PFCs (Perfluorocompounds) are used in the semiconductor industry for cleaning of dry etching and CVD (chemical vapor deposition) process. Since PFCs are global warming gases, their use is regulated by the Kyoto Protocol of 1997. GWP (global warming potential) of PFCs is 6,500-9,200 times higher than carbon dioxide, and the lifetime of PFCs is 50-200 times longer than that of carbon dioxide [1,2]. The semiconductor industry in Korea is increasing rapidly, and the consumption of PFCs is increasing sharply. The emission of PFCs in the semiconductor industry will be strictly regulated in the near future. The export of semiconductors will be reduced without a reduction of PFC emission. Therefore, PFC abatement technology must be developed. An increase in the production of semiconductors causes an increase in the use of PFC gases. The semiconductor industry cannot be grown without the PFC abatement technology.

Three technologies are used to separate or recover the PFC gases. The first method is a condensation of the gases using the difference of volatility, and it needs high power consumption to liquefy the gases to very low temperature. The second method is a membrane separation using the selective transfer of molecules by the difference of molecular size or polarity; it has difficulties in making a membrane with a high selectivity for certain molecules. When the membrane is used for a long time, the surface of the membrane can be deteriorated or the pores can be plugged. The third method is an adsorption of molecules based on the difference of affinity between gas and solid molecules. PSA (pressure swing adsorption) and VSA (vacuum swing adsorption) are the typical adsorption processes [1, 3,4]. For the purpose of PFC recovery, most researches have concentrated on the condensation and membrane separation processes, and a few researches have been reported on the adsorption processes. The power consumption of the adsorption process is relatively low, and the process can be operated without maintenance because of the long adsorbent lifetime [5-8].

Since research on PFC adsorption is in the primary stage, the selection of the proper adsorbent is required in the early stage. Isotherms are obtained from the equilibrium adsorption data, and adsorption parameters can be determined [9-15]. In order to design the adsorption bed, the dynamic behavior inside the bed must be understood by modeling and simulation. After adsorptive separation, PFC gases can be decomposed by plasma processing [16,17].

The objective of this study is to obtain adsorption and desorption characteristics to develop a process of PFC recovery in a type of cyclic operation. The adsorption profile of CF_4 inside the adsorption bed was examined by a dynamic adsorption experiment, and the desorption behavior of the strong adsorbate was examined by using the method of evacuation and purge of weak gas.

THEORY

The Langmuir isotherm was derived with the assumption of monolayer adsorption, uniform surface, no attraction between adsorbed molecules, and no mobility of adsorbed molecule:

$$q = \frac{bq_{max}P}{1+bP} \tag{1}$$

As P becomes very small, the equation is close to Henry's law of q=KP ($K=bq_{max}$). As P becomes very large, $q \approx q_{max}$. The Langmuir constant b can expressed by an Arrhenius equation,

$$b = b_0 \exp\left(-\frac{\Delta H}{RT}\right) \tag{2}$$

The adsorption is an exothermic reaction, and the sign of ΔH is minus. As the temperature increases, the value of b decreases. The temperature dependence of q_{max} is

$$q_{max} = \frac{q_0}{T^m} \tag{3}$$

†To whom correspondence should be addressed.
E-mail: nabk@chungbuk.ac.kr

The Langmuir isotherm of multicomponent adsorption can be extended as

$$q_i = \frac{b_i q_{max,i} P_i}{1 + \sum_{j=1}^{n} b_j P_j} \quad (4)$$

This equation can be used under the assumption of no interaction between adsorbed molecules. Multicomponent adsorption can be estimated from the Langmuir constant of single component [5-8].

Shock wave velocity equation was obtained from the local equilibrium model by Suh and Wankat [18], and it was used to estimate the breakthrough time by using the data obtained from the static adsorption experiment. The local equilibrium model assumes a local equilibrium between gas and solid. It neglects axial and radial dispersion, mass transfer resistance, and pressure drop. It also assumes an ideal gas, constant gas velocity, and constant temperature. The solute movement velocity can be calculated by solving the material balance equation with the method of characteristics under constant pressure. The shock wave velocity can be obtained with the assumption of no accumulation at the shock wave. The velocity equation of the shock wave can be obtained from the following equations.

$$q_i = \frac{K_i P_i}{1 + b_i P_i + b_j P_j} \quad (5)$$

$$P = \frac{p}{p_0}, \quad \phi_i = K_i \left(\frac{1-\varepsilon}{\varepsilon}\right) \rho_p R_g T \quad (6)$$

$$\xi = p_0 b_i, \quad \gamma = \frac{1+\xi_i P}{1+\xi_j P} - 1 \quad (7)$$

$$u_{sh} = \frac{(1+\gamma y_1)(1+\gamma y_2)(1+\xi_B P) u_2}{\phi_A + (1+\gamma y_1)(1+\gamma y_2)(1+\xi_B P) - [\phi_A - \phi_B(1+\gamma)] y_1} \quad (8)$$

If there is no mass transfer resistance in the bed, the period of the adsorption step can be predicted by using the shock wave velocity. The breakthrough time of the strong adsorbate can be calculated from dividing the bed length by the shock wave velocity. This estimation could be the first guideline in developing a new process.

EXPERIMENTAL

A dynamic adsorption experiment was done to obtain the concentration profile and temperature change in the adsorption bed. The feed gas was a mixture of CF_4 and N_2. The experimental conditions were room temperature (25 °C) and atmospheric pressure (1 atm), and the bed was insulated without heating and cooling. The process was vacuum swing adsorption (VSA), because the adsorption step was operated under 1 atm and the desorption step was operated under vacuum.

The apparatus for the dynamic adsorption experiment consisted of a feed section, adsorption section, and measurement section as shown in Fig. 1. The adsorption bed is 100 mm long and its inner diameter is 25 mm. The gas flow rate was controlled by mass flow controller (MFC), and the gases were mixed in the buffer tank to send to the inlet of the bed. The feed and product gases were analyzed by gas chromatography with thermal conductivity detector (TCD), silica gel column, and helium carrier gas. The analysis time was within 2 minutes, and the gas chromatogram showed the N_2 peak first and CF_4 peak next. The composition of product gases was analyzed every 2 minutes. The pressure of the bed was measured by a pressure transducer (PT) before and after the bed. A back pressure regulator (BPR) was installed after the PT to maintain the bed pressure constant. K type thermocouples were located at three positions of the bed to measure the temperature increase and the thermal wave motion. A vacuum pump was located after the sampling port to evacuate the bed during the desorption step. The maximum vacuum of the pump capacity is 5×10^{-4} torr. Activated carbon was used as an adsorbent and the properties were particle size of 20-40 mesh, BET surface area of 633 m^2/g, median pore size of 5.9 Å,

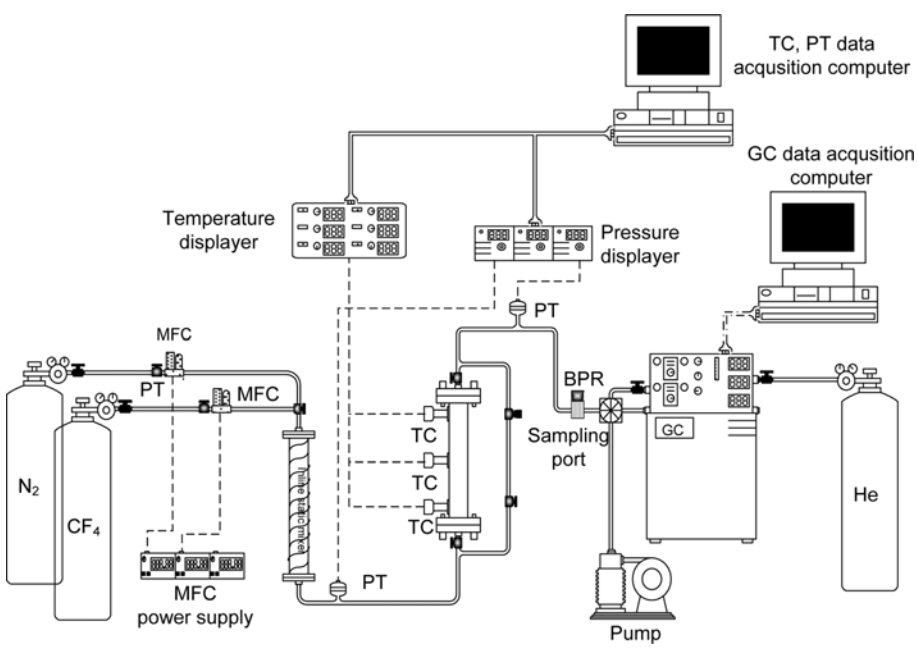

Fig. 1. Experimental apparatus for dynamic adsorption.

pore volume of 0.231 cm^3/g, particle density of 1.02 g/cm^3, and bulk density of 0.582 g/cm^3.

Before the experiment, the activated carbon was evacuated under vacuum at 150 for 10 hrs. The bed was cooled to room temperature, and it was pressurized to 1 atm by N_2. Sometimes, different gases were used instead of N_2 to test the effect of the gas. The flow rates of CF_4 and N_2 were controlled by mass flow controllers. The total flow rate of the feed gas was regulated to 100 ml/min (STP), and the concentration of CF_4 was above 1%. Before the experiment, the concentration of the feed gas was analyzed with a gas chromatograph by opening a bypass line. The adsorption experiment was started by closing the bypass line and opening the valves of the adsorption bed. The flow of feed gas was stopped when the adsorption bed was saturated with the feed gas.

After the adsorption, the flow direction inside the bed was reversed to perform the desorption experiment. During the vacuum desorption step, one valve of the bed was closed and the other valve was opened, while the bed was evacuated by the vacuum pump. For the purpose of purge, N_2 was used as a purge gas. The effect of the purge gas amount was observed with changing the N_2 flow rate. The concentration of the desorbed gas was analyzed every 2 minutes. There was no heating and cooling during the adsorption and desorption steps. The temperature changes during the adsorption and desorption were measured by three thermocouples at the bed.

RESULTS AND DISCUSSION

1. Adsorption of CF_4

The static adsorption amount was measured at 30 °C, 50 °C, and 70 °C under pressure from 0 psia to 30 psia. The adsorption amounts of CF_4 and N_2 on activated carbon are shown in Fig. 2. The data points are the experimental data and the solid lines are obtained from the fitting of the Langmuir isotherm [15]. The parameters in Eqs. (2) and (3) of CF_4 adsorption on activated carbon are obtained from the fitted data. ΔH is −4.902 kJ/mol, b_0 is 1.124×10^{-3} kPa^{-1}, q_0 is 1.35×10^5 $mol/g\cdot K^m$, and m is 3.189. These parameters are used in Eq. (8) to estimate the breakthrough time. The temperature change in the bed was smaller than 1 °C under the experimental conditions.

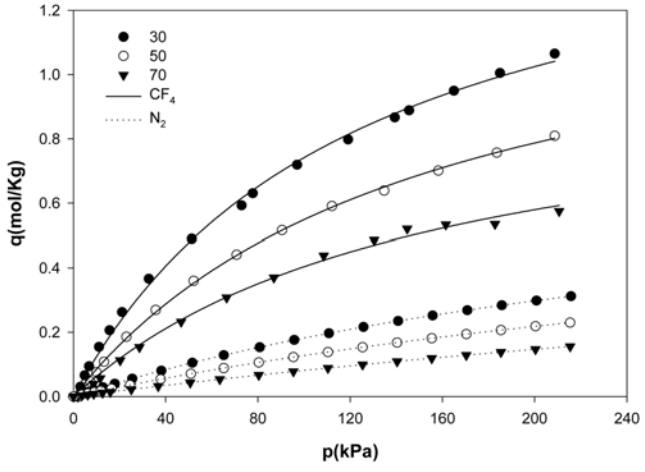

Fig. 2. Adsorption amount of CF_4 and N_2 on activated carbon 20 to 40 mesh at various temperatures.

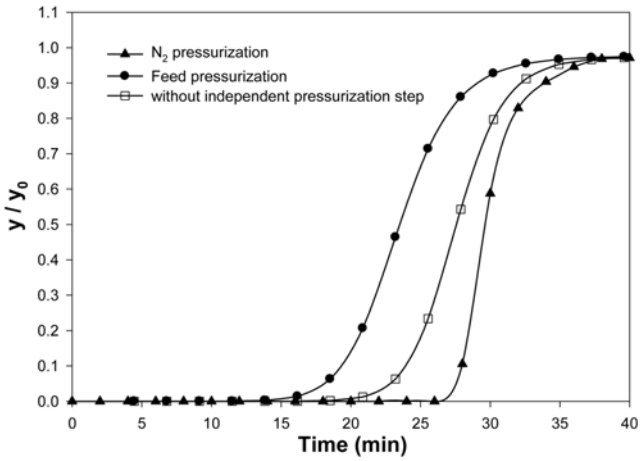

Fig. 3. Breakthrough curves of 1% CF_4 with various pressurization methods.

Therefore, isothermal operation could be assumed.

The breakthrough curves were observed depending on pressurization conditions. Three pressurization conditions were compared: N_2 pressurization, feed pressurization, and no pressurization. N_2 pressurization is a method which uses the weak adsorbate product obtained during the adsorption step. Feed pressurization is used when the amount of strong adsorbate in feed is much more than the amount of weak adsorbate or recycled amount of weak adsorbate in multibed process is small. In the no-pressurization method, there is no separate pressurization step. The feed step starts right after the desorption step terminates. The feed gas is introduced to the bed and the product gas comes out of the bed, simultaneously. The pressure in the bed increases to high pressure slowly as compared with the other pressurization methods. The no-pressurization method is similar to the feed pressurization method in the sense that there is no introduction of the weak adsorbate for pressurization of the bed.

The breakthrough curves of 1% CF4 with various pressurization methods are shown in Fig. 3. N_2 pressurization shows long breakthrough time and a steep slope. Long breakthrough time means that the amount of adsorbate is large. Steep slope means that the mass transfer zone (MTZ) in the bed is small and the adsorption is very effective. Strong adsorbate does not enter into the bed during the N_2 pressurization, so the adsorption amount becomes large. The adsorption of strong adsorbate occurs during the feed pressurization, and the adsorption amount is reduced during the adsorption step. The slope of the breakthrough curve with no separate pressurization is between the slopes of the breakthrough curves with feed pressurization and N_2 pressurization. During the feed pressurization step, CF_4 enters the bed resulting in smooth adsorbate front. From these phenomena N_2 pressurization was determined to be the effective method. In order to design a continuous process of high productivity, the N_2 pressurization method could be employed instead of feed pressurization for a mixture of feed gas of CF_4 and N_2.

The effect of CF_4 concentration on the breakthrough time is shown in Fig. 4. Feed concentration was changed to 1%, 2%, 3%, 5%, and 10%. As the concentration of CF_4 becomes high, the breakthrough time becomes short. This implies non-linear properties of adsorption isotherm. Breakthrough time was calculated from the theory of

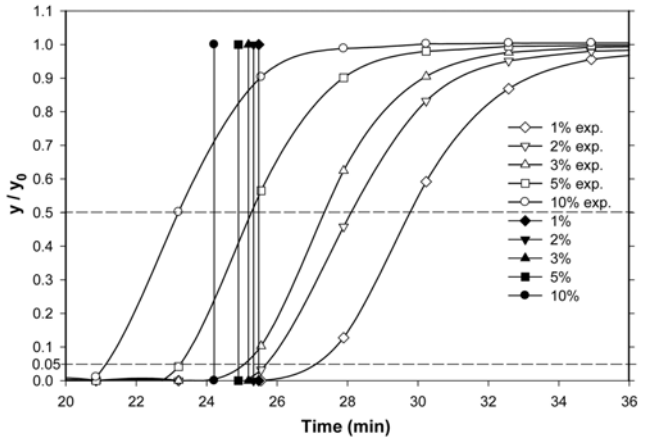

Fig. 4. Breakthrough curves of CF_4 and estimation of breakthrough time with various CF_4 feed compositions.

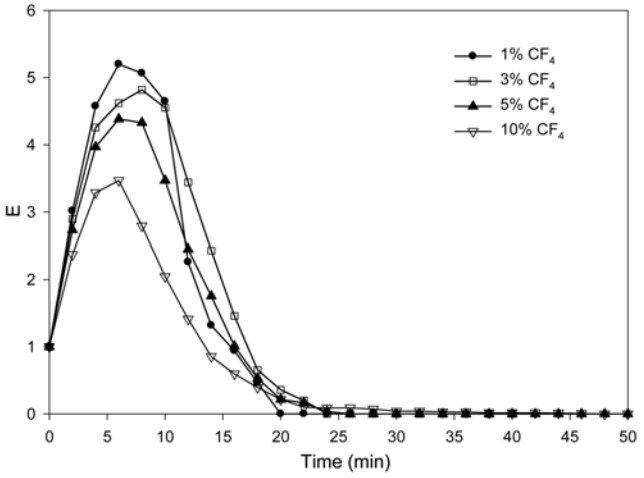

Fig. 5. Desorption curves according to various CF_4 feed compositions with N_2 purge rate of 30 ml/min under vacuum.

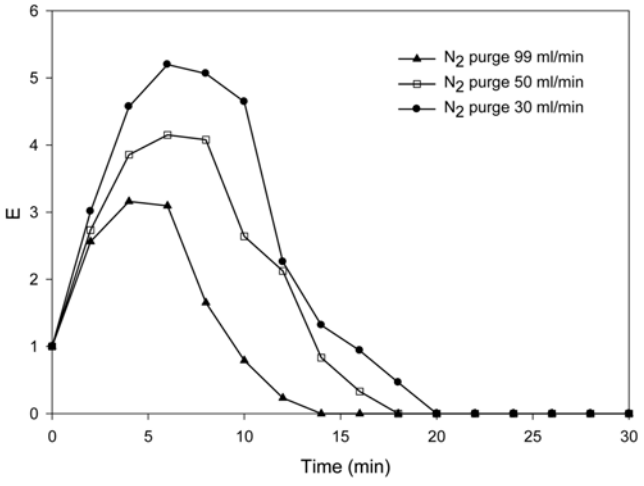

Fig. 6. Desorption curves of CF_4 according to various N_2 purge rates under vacuum for the feed composition of 1% CF_4.

the shock wave velocity equation. Since the local equilibrium model does not consider the mass transfer and diffusional resistance, the concentration profile maintains a sharp shape until breakthrough occurs. However, in real systems the concentration profile is affected by the mass transfer and diffusion, resulting in an S-shape. If the concentration profile is concentric, the time at $y/y_0=0.5$ is the same as the breakthrough time of the vertical concentration profile. In Fig. 4, experimental breakthrough curves are shown with the breakthrough times estimated by the local equilibrium model. Experimental and estimated values are similar for CF_4 adsorption. However, changes of the breakthrough times with CF_4 concentration were more significant in the experiment than in the prediction by the local equilibrium model. Therefore, mass transfer effects should be considered for modeling of the process in detail.

2. Desorption of CF_4

Changes of concentration and temperature were observed during the desorption step, which included blowdown step and purge step. The blowdown step was operated at a pressure below 1 atm. The enrichment factor (E) is the ratio of strong adsorbate concentration in the desorption product to that in the feed gas. It could be used to measure the ability of separation.

$$\text{E(enrichment factor)} = \frac{y_{i,out}}{y_{i,feed}} \tag{9}$$

As the enrichment factor becomes high, the mixture gas can be separated easily and the recovery of the desired component becomes larger.

The bed was initially saturated with CF_4 gas before the desorption experiment was performed. Feed concentrations of CF_4 were 1%, 3%, 5%, and 10%. The desorption step was N_2 purge with evacuation. The enrichment factor becomes high when the feed concentration of CF_4 is low as shown in Fig. 5. This result explains that a small change of strong adsorbate concentration in the low concentration range gives large changes of adsorbed amount. This is one indication of the nonlinearity of the adsorption curve. Nevertheless, the concentration of the outlet gas was high when the concentration of feed gas was high. The time for complete desorption was almost the same at four different feed concentrations. Therefore, in commercial operation it is not necessary to change the period of vacuum desorption when the feed concentration in upstream gas varies. It follows from this result that the diffusion rate inside the particle during desorption primarily depends on the evacuation force rather than on CF_4 concentration.

Desorption curves according to the purge gas flow rate after 1% CF_4 adsorption step are shown in Fig. 6. The pressure in the bed was increased with the increase of the purge flow rate because the bed was evacuated with the vacuum pump. As the N_2 purge flow rate increased, the enrichment factor became small due to dilution effect. However, the increase of the purge flow rate reduced the desorption time. High flow rate around particles facilitated the mass transfer of CF_4.

Figs. 7 and 8 show the desorption curves of CF_4 with separate blowdown and purge step. The bed was cleaned with weak adsorbate during the purge step. In Fig. 7, desorption curves of CF_4 with various N_2 purge rate are shown for the feed composition of 1% CF_4. For desorption, 20 min of vacuum blowdown was followed by N_2 purge under vacuum. The enrichment factor was dropped right after vacuum blowdown due to the introduction of purge gas

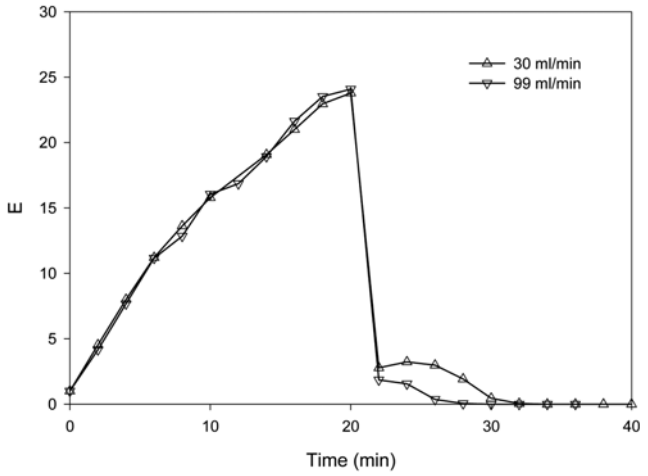

Fig. 7. Desorption curves of CF_4 with various N_2 purge rate for the feed composition of 1% CF_4; 20 min of vacuum blowdown followed by N_2 purge under vacuum.

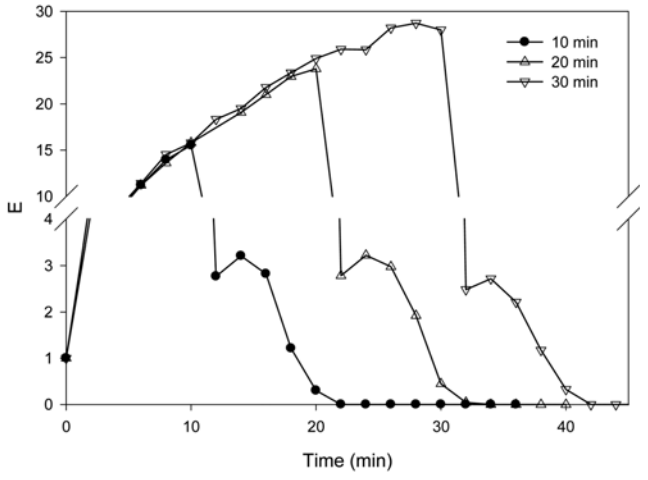

Fig. 8. Desorption curves of CF_4 with various vacuum blowdown times for the feed composition of 1% CF_4 and N_2 purge rate of 30 ml/min; vacuum blowdown followed by N_2 purge under vacuum.

resulting in dilution. As the purge gas flow rate increased, the enrichment factor became smaller and the desorption time became shorter. This result obtained for the case of purge after pure evacuation is consistent with Fig. 6 where simultaneous operation of evacuation and purge is employed. If desorption by evacuation is insufficient for complete desorption, the purge gas flow rate has the same effect regardless of the type of desorption operation.

Desorption curves of CF_4 with various vacuum blowdown time for the feed composition of 1% CF_4 and N_2 purge rate of 30 ml/min are shown in Fig. 8. As vacuum blowdown time increased without the purge gas, more CF_4 was desorbed from the adsorbent, leading to a high enrichment factor. The time between the start and end of purge for complete desorption was almost the same for three different vacuum blowdown times. As a result, operation of short vacuum blowdown time combined with large purge rate reduces the total desorption time.

The mass transfer resistance around the adsorbent particles during the evacuation without purge gas flow is higher than that in the following purge step where gas flow is introduced from the bed inlet. The longer evacuation time is, the more energy is required. The larger purge gas flow rate is, the more consumption of weak adsorbate is required. Since PSA or VSA process is a continuous process which has a cycle time and energy requirement for evacuation is significant, there is a limitation of evacuation time and the purge step is needed. Therefore, optimization of evacuation time and purge time for a given total cycle time is very important to obtain a large amount of pure product and to realize economic operation.

CONCLUSION

The adsorption amount of CF_4 and N_2 on activated carbon was measured by the static adsorption of a single component. From the adsorption experimental results it was found that CF_4 can be separated from N_2. The adsorption data of CF_4 can be fitted with the Langmuir isotherm. Langmuir constants were obtained from the temperature variation experiment, and they can be applied to the process design. The dynamic behavior of adsorbate in the bed was monitored by adsorption and desorption experiments. N_2 pressurization during the pressurization step makes the MTZ short. As the concentration of feed becomes high, the breakthrough time becomes short. This is due to the non-linearity of adsorption amount versus pressure or concentration.

The desorption of CF_4 was performed with vacuum desorption and purge with vacuum together. As the concentration of feed gas was high, the enrichment factor was low. However, the product concentration of CF_4 was high in case of high feed concentration. When the purge gas flow rate was high, the enrichment factor was low and the desorption time was short. The desorption time can be controlled by the purge flow rate. For operation of separate vacuum blowdown and purge steps, the time required for complete desorption during the purge step was independent of vacuum blowdown time. Since the mass transfer resistance around the particles during evacuation is higher than in the purge step, desorption by vacuum blowdown alone is not appropriate from the viewpoint of economics. In order to reduce the total desorption time, a short period of vacuum blowdown followed by the purge step is effective.

ACKNOWLEDGMENT

This work was supported by the New and Renewable Energy Program of MOCIE in Korea.

NOMENCLATURE

b : Langmuir constant [$psia^{-1}$]
b_0 : pre-exponential factor [$psia^{-1}$]
E : enrichment factor
ΔH : heat of adsorption [J/mol]
P : pressure [psia]
q : adsorption amount per unit mass of adsorbent [mol/g]
q_0 : adsorption amount constant [$mol/g \cdot K^m$]
q_{max} : maximum adsorption amount per unit mass of adsorbent [mol/g]

R : gas constant [$cm^3 \cdot atm/molK$]
T : temperature [K]
$y_{i,feed}$: mole fraction of gas for i component in adsorption feed
$y_{i,out}$: mole fraction of gas for i component in outlet stream

Greek Letters

γ : relative nonlinearity
ε : porosity
ξ : defined by Eq. (7)
ρ : density
ϕ : dimensionless form of the linear adsorption coefficient in Eq. (6)

REFERENCES

1. W. T. Tsai, H. P. Chen and W. Y. Hsien, *J. Loss Prevent. Proc.*, **15**(2), 65 (2002).
2. D. R. Lide, *CRC handbook of chemistry and physics*, CRC Press, 78th ed. (1997).
3. J. A. B. Van Hoeymissen, M. Daniels, N. Anderson, W. Fyen and M. Heyns, *Materials Research Society Symposium Proceedings*, **447**, 55 (1997).
4. G. M. Tom, J. McManus, W. Knolle and I. Stoll, *Materials Research Society Symposium Proceedings*, **334**, 267 (1994).
5. P. C. Wankat, *Rate-controlled separation*, Elsevier Applied Science, New York (1990).
6. R. T. Yang, *Gas Separation by adsorption process*, Butterworth Publishers, Boston (1987).
7. D. M. Ruthven, *Principles of adsorption and adsorption processes*, Wiley and Sons, New York (1984).
8. D. M. Ruthven, S. Farooq and K. S. Knaebel, *Pressure swing adsorption*, VCH, New York (1994).
9. E. Buss, *J. Chem. Soc., Faraday Trans*., **93**(8), 1621 (1997).
10. S. Tanada, N. Kawasaki, T. Nakamura, T. Ohue and I. Abe, *J. Colloid Interf. Sci*., **191**, 337 (1997).
11. S. Y. Cho and S. J. Kim, *Korean J. Chem. Eng*., **13**, 225 (1996).
12. D. J. Moon, M. J. Chung, H. Kim, B. G. Lee, S. D. Lee and K. Y. Park, *Korean J. Chem. Eng*., **15**, 619 (1998).
13. W. T. Tsai, *J. Loss Prevent. Proc.*, **15**(2), 147 (2002).
14. J. H. Yun, D. K. Choi and Y. W. Lee, *J. Chem. Eng. Data*, **45**(1), 136 (2000).
15. N. G. Ahn, S. W. Kang, B. H. Min and S. S. Suh, *J. Chem. Eng. Data*, **51**(2), 451 (2006).
16. B. K. Na, J. W. Choi, H. Lee and H. K. Song, *Korean J. Chem. Eng*., **19**, 917 (2002).
17. J. W. Sun and D. W. Park, *Korean J. Chem. Eng*., **20**, 476 (2003).
18. S. S. Suh and P. C. Wankat, *Chem. Eng. Sci*., **44**(10), 2407 (1989).